

Effect of wettability on hydrodynamics and mass transfer in small capillaries

Chaitanya Sampat^{†a,c}, Sayan Pal^{†a,b} and Amol A. Kulkarni^{*a,b}

^aChem. Eng. & Proc. Dev. Div., CSIR-National Chemical Laboratory, Dr. Homi Bhabha
Road, Pashan, Pune - 411008, India.

^bAcademy of Scientific and Innovative Research (AcSIR), CSIR-National Chemical
Laboratory (NCL) Campus, Pune-411008, India

^c Present address: Chemical and Biochemical Engineering, Rutgers University, Piscataway, NJ -
08854, USA

[†]The first two authors had equal contribution to the work

*Corresponding Author

Phone: +91-20-25902153, Fax: +91-20-25902621, E-mail: aa.kulkarni@ncl.res.in

Abstract: The wettability of the reactor wall has a significant effect on the interfacial liquid-liquid mass transfer rates in segmented flow. This work quantitatively demonstrates the importance of choosing the right material of construction of flow reactors to achieve the desired mass transfer performance. Glass and PTFE capillaries of identical diameter were used to study the effect of hydrophilic and hydrophobic surfaces on the hydrodynamics and mass transfer of the system. It was observed that for the overall mass transfer coefficient ($k_{L\alpha}$) changed by two orders of magnitude depending on the wettability of the continuous phase. The observations indicated that it is essential to achieve complete wetting of the capillary walls by the continuous phase for significant mass transfer enhancement. The observations are discussed on the basis of film thickness and slip velocity at the wall as well as the slip velocity at liquid-liquid interface. Predictions of the mass transfer coefficient using a model based on the interfacial and fluid properties showed excellent match with the experiments thereby allowing us to explore the effects of wettability on the overall mass transfer coefficient in greater detail.

Keywords: Liquid-Liquid Slug Flow, Mass transfer, Wettability, Slip Velocity.

1. Introduction

Contacting of two immiscible liquids is an important unit operation in the chemical industry. Reactors for carrying out liquid-liquid reactions (viz. in aromatic nitration, diazotization, sulfonation using oleium, Grignard reactions, etc.) and unit operations like liquid-liquid extraction are the most common examples. Most of the processes occur due to the diffusion of one phase to the other, often quantified in terms of the overall mass transfer coefficient ($k_{L,a}$, 1/m). The enhancement in the diffusion can be achieved by improving the mass transfer rates through process intensification. Among many options of process intensification, microreactors offer an order of magnitude higher values of mass and heat transfer coefficients (Burns and Ramshaw, 2001; Hartman et al., 2011; Woitalka et al., 2014) and smaller diffusion paths resulting in rapid mixing. For the liquid-liquid flow in small channels, one of the most prominent and widely used flow regimes in microreactors is the segmented flow, which is characterized by dispersed phase slugs separated by continuous phase at regular intervals. This further implies that the continuous phase wets the channel wall. Mass transfer in micro capillaries has been studied extensively in both gas-liquid and liquid-liquid segmented flows (Bercic and Pintar, 1997; Dessimoz et al., 2008; Haase et al., 2016; Raimondi et al., 2014; Van Baten and Krishna, 2004; Vandu et al., 2005). The interfacial mass transfer in segmented flow regime gets enhanced due to internal circulations in the dispersed phase (Günther et al., 2005). These internal circulations inside the dispersed phase are a result of frictional forces that are developed between the continuous and dispersed phase due to various reasons viz. flow direction, relative velocities of phases, interfacial tension, relative values of density and viscosity of the two phases, possibility of variation in the interfacial tension over the interface, etc. In general, the slip velocity between the two phases directly controls the surface renewal rate and hence the mass transfer rates.

In general, this phenomena is more evident in the case of longer liquid slugs in comparison to the shorter liquid slugs (Zaloha et al., 2012). Vandu et al. (Vandu et al., 2005) studied the effect of the capillary diameter on the mass transfer and observed an increase in the mass transfer with a decrease in the capillary diameter. This observation is primarily due to smaller film thickness in small diameter capillaries. Raimondi et al. (Raimondi et al., 2008) developed a correlation to demonstrate the effects of flow regimes and channel sizes on mass transfer in square microchannels. The mass transfer also gets affected by the flow regimes (Dessimoz et al., 2008). Recently, Zhang et al. determined the different flow patterns and segmented flow dynamics for different channel diameters and temperature, where they observed higher mass transfer rates for higher temperatures due to reduced viscosity (Zhang et al., 2019).

In microfluidic multiphase systems (i.e. G-L and L-L flows), flow regimes and velocity of individual phases are influenced by surface wetting properties of the wall (Gau et al., 1999; Santos and Kawaji, 2012; Zhao et al., 2001). The wetting properties of the fluid-wall interface are very decisive in the geometric distribution of the components of the flow. This effect becomes more prominent as the channel size decreases. The wettability of a liquid on a solid surface can vary significantly based on the surface energy of the solid which is an intrinsic property of the wall material of the channel and is usually quantified in terms of contact angles. Though contact angle depends on several parameters such as surface roughness (nodular and fibrous surface structure), impurities, surface chemistry and temperature, it is primarily a function of surface chemistry (Kuhn et al., 2011) (Ahmmed et al., 2016). In order to acquire ordered flow pattern, tweaking the respective contact angle was widely reported in the literature by means of modifying the wetting properties of the channel walls (Oskooei and Sinton, 2010) and surfactant addition into the continuous phase at different concentrations (Xu et al., 2006). When the dispersed phase slug or bubble displaces a continuous wetting fluid in microchannels, a liquid film is deposited between the dispersed phase slug and the channel wall surface. Under varying wettability conditions between the solid wall surface and the liquid, shear flow, dewetting due to surface inhomogeneity, the liquid film formation surrounding the dispersed phase slug or bubble may occur irregularly, resulting in a partial wetting condition (Srinivasan and Khandekar, 2017). In literature, the wetting and non wetting cases of gas-liquid slug flow are referred as wet and dry slug flow, respectively (Lee and Lee, 2008; Srinivasan and Khandekar, 2017).

Among the various methods for the estimation of the mass transfer, some took into account only the slug cap contribution for mass transfer (Bercic and Pintar, 1997) while on the other hand, a majority of it considered the contribution of the film for the mass transfer (Vandu et al., 2005). The models which took into account both the film and the bubble cap contribution usually tended to overestimate the values, whereas the models based on only bubble cap contribution tended to underestimate the mass transfer coefficient (k_{La}) value (Raimondi et al., 2014). The flow patterns inside the liquid film in slug flow has significant effect on the hydrodynamics and mass transfer (Ghaini et al., 2011; Matsuoka et al., 2016). In the aforementioned literature, the importance of mass transfer happening in the film section of the slugs was reiterated. The variation in pressure drop due to the effect of channel inner wall wettability in gas-liquid flow has been reported by several authors (Cubaud et al., 2006; Lee and Lee, 2008; Rapolu and Son, 2007). Hydrophilic, hydrophobic and superhydrophobic

channels have been characterised with different pressure drops (Rapolu and Son, 2007) and the later is reported for drag reduction in gas-liquid flow (Ou et al., 2004; Song et al., 2014).

Zhao et al. have observed a three-fold increase in the mass transfer coefficient which changing surface properties for multiphase flow in microchannels (Zhao et al., 2010). However, their findings cover the parallel/annular flow regime. Furthermore, for liquid-liquid segmented flow, a phase inversion happens with hydrophobic channels while in gas liquid segmented flow the liquid phase stays the continuous phase showing partial wetting behaviour. In addition to that, the viscosity of the dispersed phase liquid slug, which corresponds to the gas bubble in the case of gas-liquid flow, stays no longer negligible and also plays a significant role in the frictional pressure drop in liquid-liquid segmented flow (Kim et al., 2014). Though several correlations have been reported for estimation of mass transfer coefficients, they do not take into account the implications of varying wettability on mass transfer performance, and it needs to be studied extensively for choosing the material of construction of the micro and mini reactors.

It can be apprehended from the literature that wettability and surface tension regulates the ease with which the slugs travel throughout the channels and further knowledge of these effects on slug flow is required for designing micro and mili reactors to ensure required mixing performance. In the present work, two capillaries of the same inner diameter but having different wettability properties was used, such that the effects of the adhesion of the continuous phase on the capillaries could be studied and in turn how these forces affect the mass transfer. Effect of wettability change on flow regime, pressure drop and slug velocities was also studied in order to have a better understanding of the effect on the mass transfer. Mass transfer performance has been studied with respect to the slug velocities and the energy dissipated in the system (i.e. power consumption) based on which a recommendation is made on selecting the material of construction of the flow channels. Finally, an empirical model is developed to quantify the effect of wettability and physical properties of the multiphase system on mass transfer in small capillaries. The purpose of this work is to shed light on the effect of wall wetting on the mass transfer behaviour of the microfluidic segmented flow.

2. Experimentation and data analysis

2.1. Experimental Setup

The experimental setup consisted of a straight capillary, two syringe pumps (Holmarc Opto-Mechatronics, HO-SPLF-1), a digital manometer (HTC PM-6205, 0.01- 34 kPa), a pair of conductivity probes (made of copper wires with a tip size of 0.2 mm connected at the end of the capillary) connected to a conductivity meter and a data acquisition system connected to a computer. A schematic view of the setup is shown in Fig 1. Hydrodynamics in two types of capillaries were investigated in the experiments, one made from glass and the other made from Polytetrafluoroethylene (PTFE) (Cole Parmer, USA), both having the same internal diameter of 2.12 mm and the length (0.7 m). Each capillary has a volume of $2.43 \times 10^{-6} \text{ m}^3$ (i.e. 2.43 ml). To investigate the mass transfer in liquid-liquid system, two immiscible non-reacting systems of water-kerosene and water-toluene (Thomas Baker) were used. Propionic acid (HiMedia, India) was used as the solute. The extraction of propionic acid from the organic phase to the aqueous phase was monitored to estimate the interfacial mass transfer. A stock solution of the organic phase was made by adding propionic acid to the organic solvent in the ratio of 1:4 v/v (3.34 moles/litre). A stock solution of the aqueous phase was made by adding 10 ml of propionic acid to 10 L of water (0.013 moles/litre). This stock solution of the aqueous phase was used for all the experiments. This addition of propionic acid ensured that the initial conductivity of water was constant throughout the experiments.

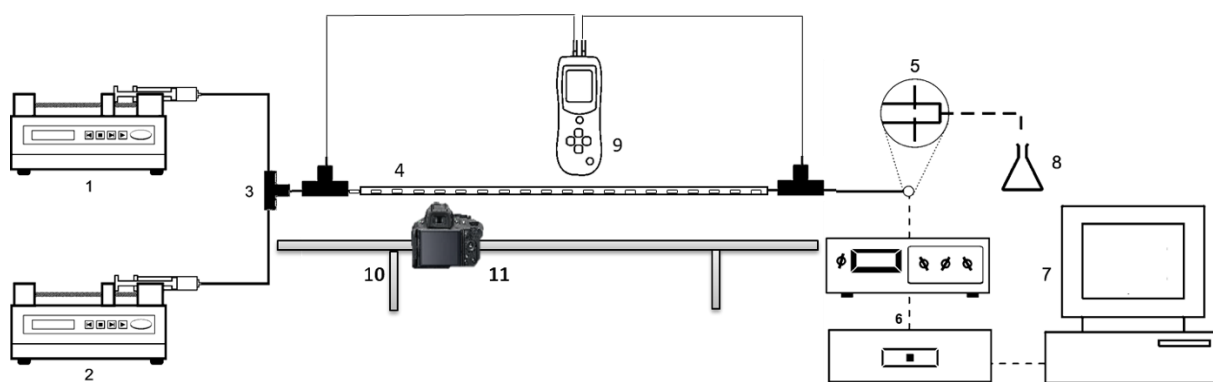


Fig. 1. The experimental setup. 1 & 2 - Syringe Pumps, 3 - T-junction, 4 - Capillary, 5 - Conductivity probe, 6 - Conductivity meter and Data translation unit, 7- Computer, 8 - Outlet collection, 9 – Manometer, 10 - Camera Rail, 11 – DSLR Camera.

The organic and aqueous stock solutions were pumped using syringe pumps (Holmarc Optoelectromechano Systems, India) separately, and the pump outlets were connected to a T-junction. The flow rates of both the phases were varied from 0 – 20 ml/min. The volumetric

flow ratios of the two liquids were varied in from 1:16 to 16:1 (Organic: Aqueous). The aqueous solution was pumped initially inside the system and once steady flow was reached the organic stock solution was pumped. Steady state was assumed to be reached when the flow of both solutions was kept running for at least five times the residence time for the total flow rate inside the capillary. The experiments were carried out at room temperature (~ 25°C). The capillaries were illuminated from behind using a light source and a diffuser. A Sony DSLR high-resolution camera was used to record the flow at 30 fps, which was subjected to further analysis. The capillaries were subjected to cleaning between each experiment with a solution consisting of Sulphuric acid and Nitric acid to remove any remnants from previous experiments.

2.2. Measurement Techniques

2.2.1. Measurement of the mass transfer coefficient

The conductivity meter was calibrated for various concentrations of the propionic acid in water up to its equilibrium concentration. The equilibrium concentration (C^*) was determined by keeping the stock solutions in constant stirring condition for two hours. Conductivity was measured online by attaching the conductivity probes at the capillary end and using a data translation unit connected to a computer for further analysis (See Fig. 1). The mass transfer coefficient was estimated using the following equation:

$$k_L a = \frac{1}{t} \ln \frac{C^* - C_{in}}{C^* - C_{out}} \quad (1)$$

, where C_{in} , C_{out} and C^* are the concentrations of propionic acid in the aqueous phase at the inlet and outlet and the equilibrium concentration respectively, t is the mean residence time, and $k_L a$ is the overall mass transfer coefficient (Sharma et al., 2017). The values of conductivity for specific concentrations were also confirmed by carrying out experiments involving water-air system by dissolving known concentration of propionic acid in water. 5 different concentrations over the range of 0.5 mol/L to 2 mol/L were prepared and experiments were carried out by flowing the two phases in glass capillaries. The measured conductivity was compared with the original conductivity from bulk solutions and the variation was less than $\pm 2.4\%$, which is not very significant.

2.2.2. Pressure drop measurement and conductivity meter calibration

A digital manometer (HTC Instruments PM-6205) was connected to the start and end of the capillary using T-junctions to measure the pressure difference between the two points. The

pressure drop was recorded online for a range of flow rates as the manometer was connected to a computer.

The concentration of the resulting solution was measured using two terminals inserted at the end of the capillary using 2 metal pins. It was made sure that the terminals did not touch each other during the span of the experiment. The transient conductivity meter reading showed highest and lowest peaks which accounts for the aqueous (conductive) and organic (nonconductive) phase slugs coming in contact with the terminals respectively (See Fig.S1 in the supporting information for further details). A MATLAB code was developed to estimate a mean steady state value of the conductivity and concentration from the highest peaks. Every experiment was repeated three times and a three-point validation of conductivity meter was done ensuring that it is within the calibration curve. Fig. S2 in the Supporting Information shows the calibration curve used to predict the concentration as a function of reading on the conductivity meter.

2.2.3. Determination of slug length, velocity and specific interfacial area

The images of the two-phase flow in the capillaries were analysed using the image analysis software ImageJ. Each image was individually calibrated using the diameter of the capillary as the known scale. The slug length was determined by measuring the distance between the two extreme ends of each slug. The slug was then divided into three sections viz. one cylindrical section (in the middle) and two hemi-ellipsoidal sections (at each end of the slug) as shown in Fig 2. The surface areas of each of these sections were calculated, and the slug volume was also estimated for each slug. Thus, the specific interfacial area was calculated by dividing the total surface area of the slug by the slug volume. Videos of slug flow were recorded by focusing the camera at a fixed known distance of 25 mm from the inlet of the capillary. The videos were then subjected to analysis using the Tracker 5.0 software ([Open Source Physics](#)) where the average velocity of the slugs was determined using the in-built tracker module.

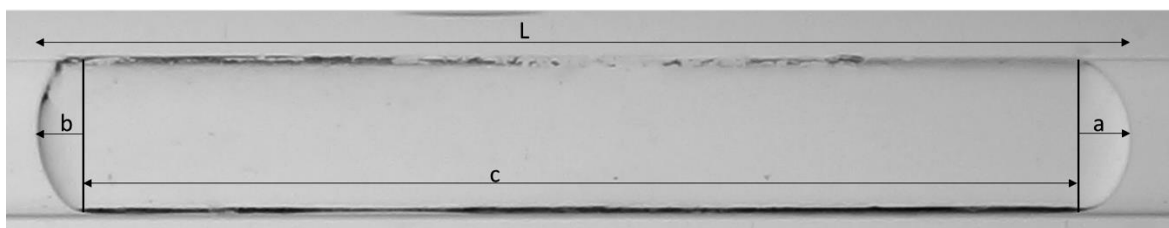


Fig. 2. Division of the slug for interfacial area measurement. L is the length of the slug, a & b are the radii of the front and rear semi-ellipsoids respectively, and c is the length of the cylindrical section.











	Kerosene - Glass	Toluene - Glass	Kerosene- Teflon	Toluene - Teflon
Uniform Slug Flow	 $Q_W = 0.2 ; Q_K = 0.1$	 $Q_W = 0.1 ; Q_T = 0.2$	 $Q_W = 0.5 ; Q_K = 0.5$	 $Q_W = 1 ; Q_T = 1$
Parallel Flow	 $Q_W = 20 ; Q_K = 20$	 $Q_W = 12 ; Q_T = 12$	Not Observed	 $Q_W = 15 ; Q_T = 15$
Stagnant Boundary Layer	 $Q_W = 0.25 ; Q_K = 0.5$	 $Q_W = 0.5 ; Q_T = 0.5$	 $Q_W = 1.75 ; Q_K = 1.75$	Not Observed

Fig. 3. Different types of flows observed in 2.12 mm diameter capillary (All flowrates Q are in mL/min, subscripts W – water, K - kerosene)

3. Results and Discussion

The wettability of the aqueous phase is better on glass capillary and very poor on the PTFE capillary. The organic phase showed better wettability than water for the PTFE capillary. The physical properties and contact angles for kerosene, toluene, propionic acid and water are listed in Table 1. The contact angle of kerosene and toluene stock solutions (with Propionic acid) can

Table 1. Physical Properties and contact angles of the pure phases on Glass and Teflon (Fox and W.A., 1950; Kitamura et al., 1992; Saien and Akbari, 2006; Yuan and Lee, 2013)

	Physical Properties			Contact angle (θ^0)	
	Density ($\rho, \text{kg/m}^3$)	Viscosity ($\mu, \text{Pa.s}$)	Interfacial Tension ($\sigma, \text{N/m}$)	Glass	Teflon
Kerosene	810	0.00162	0.048	26	46
Toluene	867	0.000551	0.0371	12	43
Water	1000	0.001	0.0728	5	108 - 114
Propionic acid	990	0.00102		35	70-85

Table 2: Flow regimes observed at different flow rates and capillaries. (S: Slug flow, P: Parallel flow, T: Transient regime. For certain flow rate ranges, the flow regime was seen to switch between slug flow and parallel flow in an unsteady manner and hence defined as Transient regime.) (Capillary wetting wall and continuous fluid combination: G-K: Glass-Kerosene, T-K: Teflon-Kerosene, G-T: Glass-Toluene and TT: Teflon-Toluene)

Flow rate (ml/min)		Disperpased phase holdup (-)	Capillary wetting wall: Wetting fluid			
Continuous phase	Dispersed Phase		G-K	T-K	G-T	T-T
0.1	1	0.91	S	S	S	S
0.1	0.1	0.50	S	S	S	S
0.2	1	0.83	S	S	T	S
0.2	0.2	0.50	S	S	S	S
0.2	0.1	0.33	S	T	S	S
0.4	0.4	0.50	S	T	S	S
0.5	8	0.94	S	S	T	T
0.5	7	0.93	S	S	S	T
0.5	6	0.92	S	S	S	S
0.5	4	0.89	S	S	S	S
0.5	2	0.80	S	S	S	S
0.5	1	0.67	S	S	T	S
0.5	0.5	0.50	S	S	S	S
0.75	0.75	0.50	S	T	S	S
1	1	0.50	S	T	S	S
1	0.5	0.33	S	S	S	S
1.25	1.25	0.50	S	S	S	S
1.5	1.5	0.50	S	S	S	S
1.75	1.75	0.50	S	S	S	S
2	2	0.50	S	S	S	S
2	1	0.33	S	T	S	S
2	0.5	0.20	S	S	S	S
4	0.5	0.11	S	S	T	S
5	5	0.50	S	T	S	S
6	0.5	0.08	S	S	T	S
7	0.5	0.07	S	S	T	S
8	8	0.50	P	S	P	S
8	0.5	0.06	S	S	T	T
9	9	0.50	P	T	P	S
10	10	0.50	P	S	P	S
12	12	0.50	P	P	P	S
15	15	0.50	P	P	P	P
20	20	0.50	P	P	P	P

be assumed to be in between the contact angles of pure solvent and that of the propionic acid. This is a safe assumption as this small variation does not change the wetting properties of the solution significantly with respect to the capillary walls.

In a glass capillary, the aqueous phase formed the continuous phase while the organic phase formed the dispersed phase. The propionic acid diffused from the dispersed phase slugs to the

continuous phase. On the other hand, the organic phase was observed to wet the PTFE capillary due to the hydrophobic surface (see Fig. 3). The flow regimes observed in these sets of experiments were slug flow, wavy parallel flow and parallel flow. The latter two flows were only observed for very high flow rates (total flow rate > 10 ml/min) in the kerosene-water system. The effect of viscosity could not be neglected here since the toluene-water system having relatively lower viscosity and tended to produce wavy and parallel flow at lower flow rates in comparison to the kerosene-water system. A stagnant film was observed to be trapped between the dispersed phase slug and the capillary walls predominantly for glass capillaries. The comparison of different types of flows is shown in the images in Fig. 3. Table 2 provides an exhaustive list of flow regime observed for all the experimental studies conducted in this work.

3.1. Effect of wettability on hydrodynamics

Initially, we have studied the effect of wettability change on pressure drop, slug velocity, slip length and hence the boundary layer considerations for both the capillaries. As discussed previously, the aqueous phase completely wets the glass capillary, whereas in the case of PTFE capillary, the organic phase only partially wets it. In general, the pressure drop was found to be higher in glass capillary than for the PTFE capillary. The complete wetting of the glass capillary by the continuous phase (here aqueous phase) led to no-slip condition, thereby experiencing relatively higher frictional resistance. While in the case of the PTFE capillary, the extent of wetting by the organic phase was much lower (See contact angles in Table 1) resulting in relatively lower frictional resistance at the wall. For the case of partial wetting, when liquids are forced to move over the wall surface, it is energetically favourable not to wet the surface. The variation in pressure drop across the capillaries for a range of flow rates of different organic-aqueous phase combinations is shown in fig. 4. The effect of the wettability in four types of experiments is discussed subsequently. In general, the pressure drop increases with the increasing Re , due to the increase in the frictional pressure drop. At low flow rates ($1 < Re < 100$), the variation in the pressure drop was indistinguishable as the inertial effects were not very prominent (see Fig. 5). For all the studies presented the Reynold's number for the system was calculated using the volume average fluid properties as follows:

$$Re = ([Q/(\pi d^2/4)] * \bar{\rho} * d) / \bar{\mu}$$

, where, Q is the total flow rate as calculated in Table 2, d is the capillary diameter, $\bar{\rho}$ is the weighted average density for the system and $\bar{\mu}$ represents the average viscosity of the system.

The average values of physical properties were obtained on the basis of volume fraction of phases.

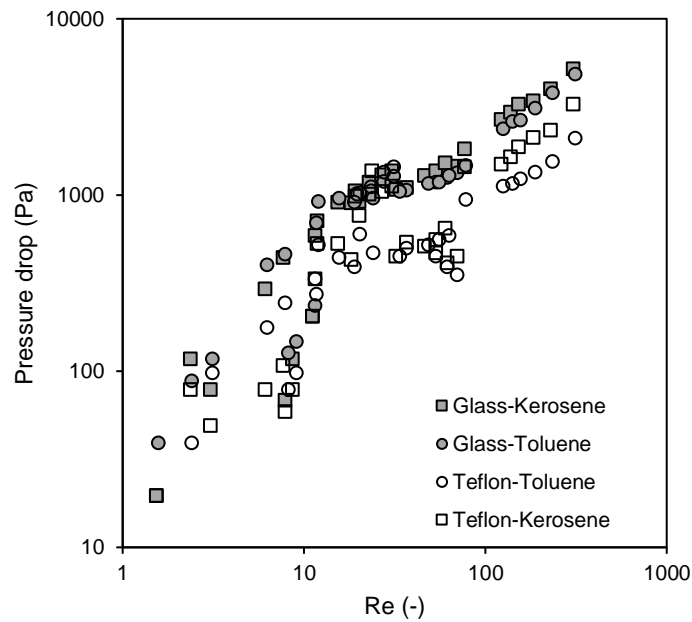


Fig. 4. The variation in pressure drop in glass and PTFE capillaries with Reynolds Number for both systems, Kerosene and Toluene for $Re = 1 - 1000$. (Filled and empty data points represent wetting and non-wetting cases respectively)

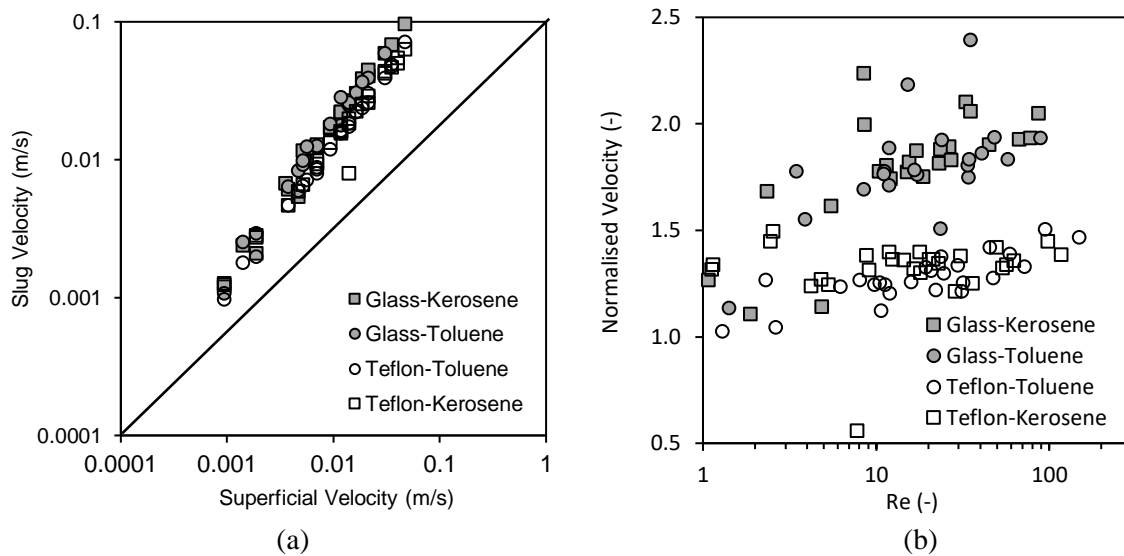


Fig 5. Experimental measurements: (a) Experimentally measured slug velocity vs. superficial velocity; (b) Normalized slug velocity (Measured slug velocity/Superficial velocity) as a function of Re .

However, at higher flow rates ($100 < Re < 1000$), the pressure drop increased almost linearly with Re (see fig. 4). The pressure drop variation in the glass and teflon capillaries were observed to be different thereby confirming that the wetting of the capillary by the continuous phase plays an important role here. The pressure drop for the wetting glass capillary was observed to be always higher when compared to that of for the PTFE capillary (Fig. 4). In the literature, fluid velocities in hydrophilic and hydrophobic microchannels are measured by μ -PIV for

aqueous solutions and a significant fluid velocity is reported near a hydrophobic microchannel wall while no-slip condition prevails for a hydrophilic surface (Tretheway and Meinhart, 2002). The higher extent of wetting an no-slip boundary conditions in hydrophilic capillaries accounts for the relatively higher frictional resistance and subsequently higher pressure drop. The toluene-water system showed an affinity for parallel flow instead of segmented flow at higher flow rates, and this resulted vividly in a lower pressure drop than the kerosene-water system at the said conditions.

As slug flow was observed over most of the experimental conditions, it would be interesting to understand the effect of contact angle or extent of wetting by the continuous phase on the dispersed phase slug velocity. The extent of wetting would determine whether the slug is decelerated or accelerated. Fig. 5a compares the slug velocities obtained from the experimental data with the calculated superficial velocities. The difference from the parity line indicates the role of wettability as well as physical properties of liquids. This deviation in the velocity can be attributed to the slip experienced by the continuous phase on the inner walls of that capillary (Choi et al. (2003)). In order to identify the actual controlling parameters, the slug velocities were normalized by the total superficial velocity (Fig. 5b), which was seen to remain a strong function of the Re . The normalised velocities for the glass capillaries were observed to be always higher than the PTFE capillary indicating the adhesion forces between the continuous phase and the capillary walls have a more significant influence on the slug velocity than the physical properties. Enhancement in the value of normalized velocity for glass capillary was higher due to better wetting of the wall surface characterised by the significantly lower contact angle of wetting aqueous phase (Cubaud et al., 2006). Thus skin friction would lead to enhanced shear stress on the interface between two fluid phases, thereby resulting in stronger internal circulation in the slugs. Thus, the internal circulation rate in the dispersed phase, which actually depends on the slug velocity is strongly governed by the wetting properties. This implies that the behaviour of the interface, including the slip conditions at the wall is varied.

A definition of the boundary conditions is necessary to explain this phenomenon. There are three types of widely accepted boundary conditions: no-slip, true slip and apparent slip, which are represented in a schematic in fig. 6. Under no-slip and apparent slip, the relative velocity between the fluid and the capillary wall is zero at the wall. For the later case, liquid slips on top of a thin layer of liquid attached to the solid wall (shaded region). For the case of true slip boundary condition, slip occurs at the wall with non zero velocity of the fluid.

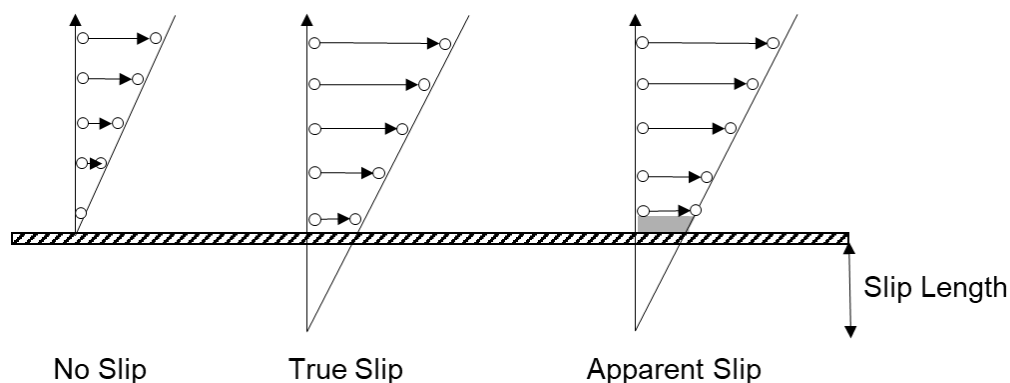


Fig 6.Type of boundary conditions at capillary walls. (Neto et al., 2005; Ou et al., 2004)

Since the observations from the glass capillary showed the presence of a stagnant layer of the continuous (aqueous) phase, and there was a presence of slip as indicated by the deviation in slug velocities, thus only the apparent slip boundary condition (stagnant layer) is applicable in glass capillaries. The organic phase partially wetted the PTFE capillary forming a very thin film at the inner walls of the PTFE capillary. This organic layer formed in the PTFE capillary was not stagnant like the film formed by the aqueous layer in the glass capillary. Thus, in the PTFE capillary, the boundary condition observed was that of the true slip, where the velocity of the continuous phase was not zero at the inner walls.

While the wettability at the wall controls the slip velocity of the fluid in its vicinity, another parameter that also plays a significant role in interfacial mass transfer is the slip at the interface between two phases. This specific slip also contributes to the shear rate inside the film and hence the mass transfer across the film. For example, when the flow rates of both the fluids are identical and when one of the phases wets the wall such that it has no slip at the wall, the film thickness will be governed by the capillary number and the fluid viscosity. Considering that the system follows a segmented flow regime, the finite thickness of the continuous phase will push the dispersed phase away from the wall thereby resulting in slugs of aspect ratio > 1 . In such a situation, the dispersed phase slug will move at a superficial velocity, which will be based on the flow area available after excluding the film thickness. Thus, the velocity difference between the continuous phase film and the dispersed phase will result in a slip at the interface, which will be prominent when the continuous phase wets the wall. For the case where wettability is relatively less, the slip at the wall by the film of continuous phase will reduce the slip at the other side of the film, i.e. the interface between the continuous phase and the dispersed phase. This further reduces the shear rate in the film and thus would reduce the extent of mass transfer. We have depicted these cases in the Supporting Information S2.

3.2. Effect on Mass Transfer

The overall mass transfer coefficient ($k_L a$) is affected by various factors like specific interfacial area, flow rates, flow regime and slip conditions. Mass transfer between the two phases has a significant dependence on the motion of the interface as well as the interfacial area for the diffusion of the solute to occur. The nature of internal circulation in the dispersed phase slug depend upon the interfacial tension, slug length and the relative values of density and viscosity of the two phases. Here we have focused on the role of wettability on interfacial mass transfer rates. The adhesion of the continuous phase to the inner walls of the capillaries plays an important role in determining the amount of mass transfer occurring between the phases. The variations of the mass transfer coefficient ($k_L a$) observed with these factors are discussed, and a model for estimation of the $k_L a$ based on the contact angle and physical properties was developed.

3.2.1. Variation of $k_L a$ with slug velocity and film thickness

The mass transfer between the dispersed and the continuous phase occurs due to the concentration gradient between the two phases. It is reported in the literature that the mass transfer coefficient increases with the increase in slug velocity (N. Kashid et al., 2011). Our experiments also showed a similar behaviour (see fig. 7). Smaller slugs were observed at higher flow velocities due to early detachment of droplets, which indicated a higher interfacial area available for mass transfer (Ghaini et al., 2010). At identical velocity, for both, kerosene-water and toluene-water systems the $k_L a$ was observed to be higher in the case of glass capillary than in PTFE capillary, primarily because of the slip variation. The lesser extent of wetting by the organic phase resulting in relatively lower frictional resistance at the PTFE accounts for the decrease in the mass transfer coefficient. The hydrodynamic friction factor is expected to have increased due to higher wettability (Srinivasan and Khandekar, 2017). For the hydrophilic surface, the mass transfer coefficient was almost independent of the dispersed phase. However, for the hydrophobic surface, higher mass transfer was observed for the toluene-water system.

The rate of diffusion is governed by the extent of circulation in the dispersed phase and the shear in the continuous phase film surrounding the slug (Burns and Ramshaw, 2001). The effect of wetting on film thickness was reported by Stokes (Stokes, 1966). The difference between the film thickness between the two systems can be attributed to the difference in the physical properties of the same. The mass transfer coefficient was plotted against the estimated film thickness, and it was found to increase irrespective of the capillary wall and the multiphase

systems (See supporting information S3). As the resistance to the dispersed phase motion from the film increases, the internal circulations inside the slug also increase, thereby leading to enhanced mass transfer rates. The mass transfer for the same film thickness was higher in the case of the glass capillary due to the complete wetting of the glass and the interfacial tension between the slug and the film. On the other hand, in a PTFE capillary, the wetting layer was not stagnant due to partial wetting, thereby offering relatively lower resistance to flow of the slug. A relatively thinner film in the PTFE capillary would have reduced the extent of circulation in the slugs resulting in the lower interfacial mass transfer.

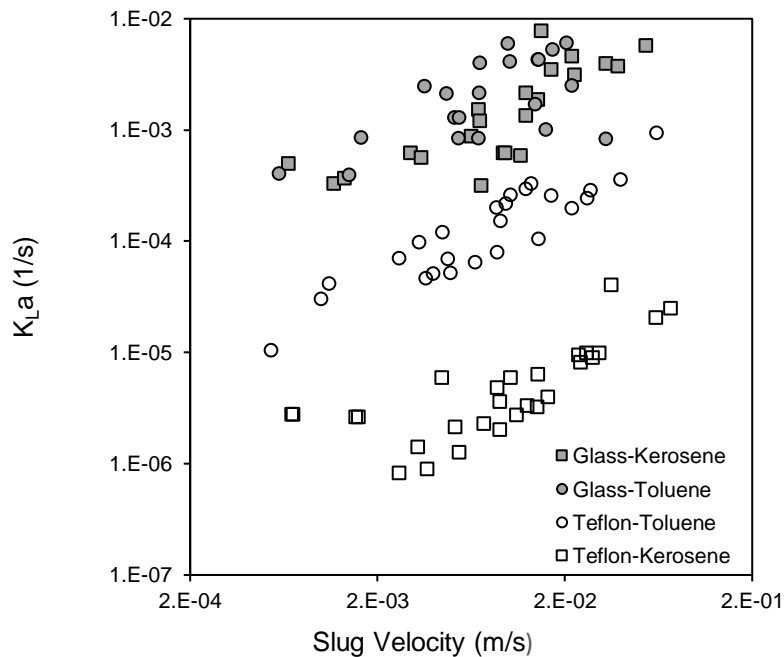


Fig. 7. Overall mass transfer coefficient as a function of slug velocity

In general, higher film thickness implies greater friction and hence, increased pressure drop. Thus, at a fixed flow rate, situations leading to higher film thickness would lead to better mass transfer due to relatively higher levels of energy dissipation rates. It was also observed in our experiments and reported literature (Ghaini et al., 2011; Khan et al., 2017) that slug lengths in wetting capillaries are lower in comparison to partial wetting capillaries. This smaller size of slugs also enhances circulation intensity in wetting channels resulting in better mass transfer performance. The results are in agreement to Butler et al. (Butler et al., 2018), where the authors observed an increase in the film thickness and its exchange with the continuous bulk phase can lead to the increase in the mass transfer coefficient even though the fluid viscosity is increased and the recirculation is reduced.

3.2.2. Variation of $k_L a$ with Pressure Drop

The variation in mass transfer coefficient with pressure drop of the system was studied, which gives an idea of the mass transfer efficiency at varying channel surface wettabilities from the energy point of view. The presence of a wetting film at the wall gives additional resistance to the flow, thereby increasing pressure drop across the channel. In a previous Section (3.1) it was discussed that for hydrophilic capillaries, higher frictional resistance also induces relatively intense internal circulation in the dispersed phase as well as the continuous phase, thereby enhancing the mass transfer rates.

Fig. 8 illustrates the variation of the mass transfer coefficient with the total power consumed, estimated as a product of pressure drop and flow rate, i.e. $W = \Delta P \cdot Q$. A steady rise in the value of $k_L a$ with increasing energy input was observed irrespective of the capillary wall material and the dispersed phase. At identical power consumption, the hydrophilic glass capillary always resulted in higher mass transfer coefficient. This is due to the better wetting behaviour, the shear rate in the liquid film between the dispersed phase slug and the wall increases for the same power consumption. At higher flow rates of toluene, a drop in the mass transfer coefficient was observed inside the glass capillary, which corresponds to a flow regime change from slug flow to parallel flow, where mass transfer decreases due to lesser interfacial area and missing internal circulations. It can be concluded that the surface wettability affected the distribution of the two liquid phases inside the channel and played an important role in energy dissipation, and eventually resulted in a significant difference in mass transfer.

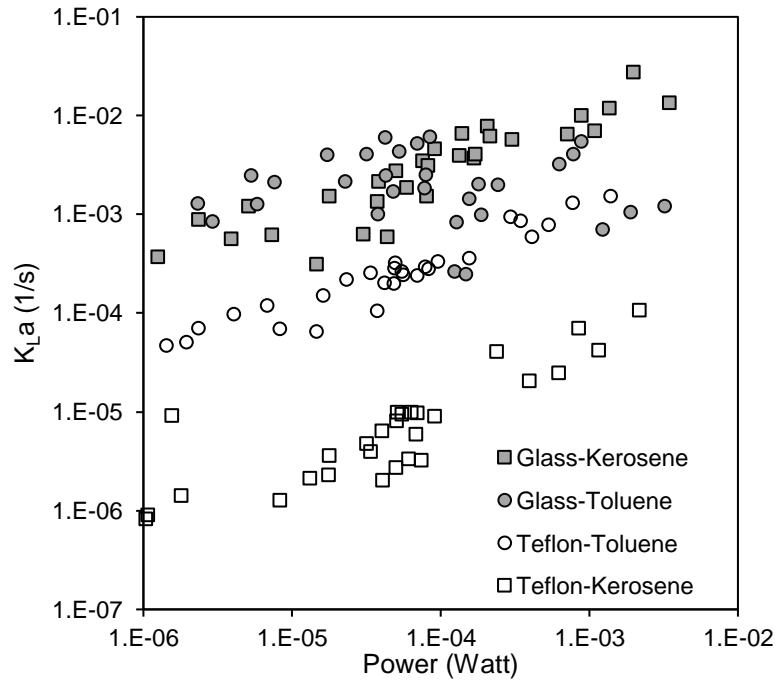


Fig. 8 : Overall mass transfer coefficient v/s power consumed.

3.2.3. Correlation for mass transfer coefficient

In order to get a deeper insight of the mass transfer behaviour in the form of dimensionless numbers, the overall $k_L a$ was used for the estimation of Sherwood number (Sh), which is a dimensionless expression of the mass transfer coefficient. Sh was plotted as a function of the product of Re and Ca . The trend could be correlated in the following form (Eq. 3-5) where the intercepts were seen to be a strong function of the contact angle and physical properties. The indices of the dimensionless numbers in the correlation were determined by means of non-linear regression analysis. Coefficients were optimised by calculating the sum of square errors between the predicted and the actual experimental data.

$$Sh = a(Re. Ca)^{0.35} \quad (3)$$

$$\log Sh = \log a + 0.35 \log Re. Ca \quad (4)$$

$$\log a = (\gamma)^{-2.57} \left(\frac{\rho_d}{\rho_c}\right)^{38.98} \left(\frac{\mu_d}{\mu_c}\right)^{2.68} (\cos\theta)^{54.51} \quad (5)$$

Where Sh is the Sherwood number, Re is the Reynolds number, Ca is the Capillary number, γ is the interfacial tension between the two phases, ρ is the density of the phase, μ is the viscosity of the phase, θ is the contact angle of the continuous phase with the capillary walls. Subscripts c and d represent the continuous and dispersed phase, respectively. The experimental dataset

was divided into two parts and the model was developed by one dataset and validated by the other. The robustness of the fitting can be observed in fig. 9, where a parity plot comparing the Sh estimated using the fitted parameters, and the experimentally measured Sh is illustrated. Neglecting the physical properties have detrimental effects in terms of predictability and two such possibilities are presented in the Supporting Information S5.

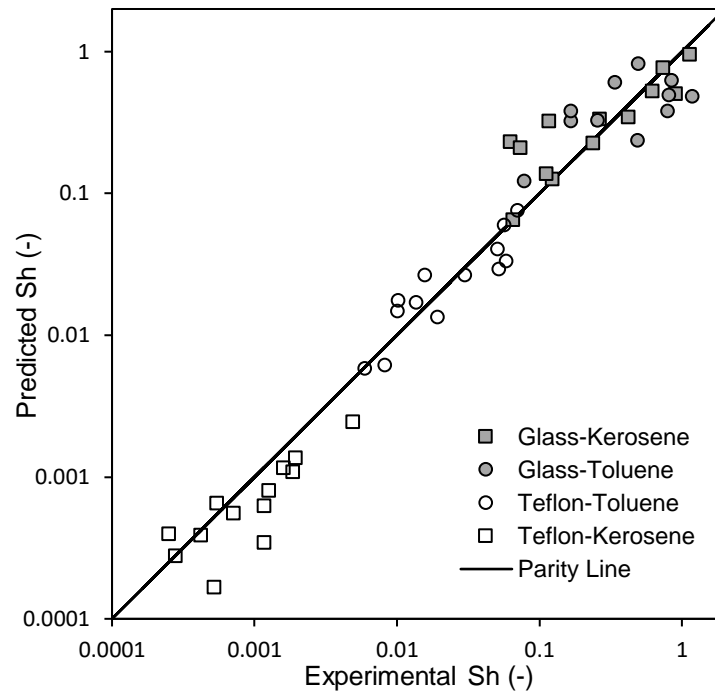


Fig. 9. Parity plot of the predicted and experimentally obtained Sherwood numbers.

The aforementioned correlation shows that the overall mass transfer coefficient depends on the inverse of interfacial tension, density ratio and the viscosity ratio. Two and three parameter models fitted for developing the correlation instead of the four parameter model in Equation 5 failed to provide a reasonable parity plot. Lower interfacial tension decreases the extent of circulation inside the slugs due to increasing resistance, while the ratio of the densities and viscosities affect the type of flow occurring inside the capillaries. Moreover, the correlation also shows that the $k_L a$ has a strong dependence on the contact angle. The contribution of the contact angle is in terms of $\cos \theta$, which varies from zero to one, which implies that the effect of the indices is significant. For example, glass and teflon capillaries have an average contact angle of 5° and 43° , which results in value of 0.8092 and 2.87×10^{-8} , respectively when substitutes for θ in $(\cos \theta)^{55.51}$. This shows that when the continuous phase completely wets the inner wall of the capillary, the mass transfer occurring is much higher in comparison to the capillary in which the continuous phase does not wet or partially wets the inner walls of the capillary.

4. Conclusions

In this study, the effect of wettability on the liquid-liquid interfacial mass transfer inside straight capillaries was studied. The wetting phenomena at the capillary walls were observed to affect the flow regime, pressure drop and slug velocities. No slip, true slip and apparent slip boundary conditions at the capillary walls were observed depending on the wettability of the system. It can be concluded from the experiments, that the wetting of the inner walls of the capillary affects the mass transfer coefficient considerably. Significant quantitative differences were observed between the interfacial mass transfer in the glass and PTFE capillaries, which indicates that the effect of wall surface wettability is important.

The continuous aqueous phase in the glass capillary formed a stagnant boundary film while in the PTFE capillary, the continuous organic phase formed a film which was in motion, i.e. it slipped on the surface of the capillary. The effect of film thickness on mass transfer was found to be significant, and with increasing thickness, the k_{LQ} increased. The wettability affects the flow characteristics as well as the hydrodynamics in a significant manner. Better wetting of the wall by the continuous phase system resulted in enhanced mass transfer, and hence it is recommended that while choosing the MOC of microchannel/capillary reactors should be wetting for the continuous phase. The slip velocity at the interface between the two fluids and slip at the wall together explain the observations and its relevance to film of the wetting phase. Very detailed flow simulations that capture these phenomena would help in giving the microscopic data on these observations. More work in this direction will be reported separately.

The obtained correlation corroborated the effect of wettability on mass transfer and the more the wetting of the capillary wall by the continuous phase higher was the mass transfer coefficient. The approximation of the mass transfer behaviour for a specific channel and for a given set of operating conditions can be established using the correlation between Sh and the product ($Re \cdot Ca$).

Notations

C_{in} inlet concentration of the aqueous phase (mol m^{-3})

C_{out} outlet concentration of the aqueous phase (mol m^{-3})

t Residence time (s)

k_{La}	Overall mass transfer coefficient (1/s)
Sh	Sherwood number (-)
Re	Reynolds number (-)
Ca	Capillary number (-)
γ	interfacial tension (N/m)
ρ	Density (kg/m ³)
μ	Viscosity (Pa.s)
θ	Contact angle of the continuous phase (°)

Conflict of interest

The authors declare that there is no conflict of interest.

Acknowledgment

Authors thank research funding from Swarnajayanti Fellowship project from DST (GoI). SP acknowledges the Council of Scientific and Industrial Research (CSIR) for providing doctoral fellowship.

References

- Ahmed, K.T., Patience, C., Kietzig, A.-M., 2016. Internal and external flow over laser-textured superhydrophobic polytetrafluoroethylene (PTFE). *ACS Applied Materials & Interfaces* 8, 27411-27419.
- Bercic, G., Pintar, A., 1997. The role of gas bubbles and liquid slug lengths on mass transport in the Taylor flow through capillaries. *Chemical Engineering Science* 52, 3709-3719.
- Burns, J.R., Ramshaw, C., 2001. The intensification of rapid reactions in multiphase systems using slug flow in capillaries. *Lab on a chip* 1, 10-15.
- Butler, C., Lalanne, B., Sandmann, K., Cid, E., Billet, A.M., 2018. Mass transfer in Taylor flow: Transfer rate modelling from measurements at the slug and film scale. *International Journal of Multiphase Flow* 105, 185-201.
- Choi, C.H., Westin, K.J.A., Breuer, K.S., 2003. Apparent slip flows in hydrophilic and hydrophobic microchannels. *Physics of Fluids* 15, 2897-2902.

- Cubaud, T., Ulmanella, U., Ho, C.M., 2006. Two-phase flow in microchannels with surface modifications. *Fluid Dynamics Research* 38, 772.
- Dessimoz, A.L., Cavin, L., Renken, A., Kiwi-Minsker, L., 2008. Liquid–liquid two-phase flow patterns and mass transfer characteristics in rectangular glass microreactors. *Chemical Engineering Science* 63, 4035-4044.
- Fox, H.W., W.A., Z., 1950. The Spreading of Liquids on low energy surfaces. *Journal of Colloid Science* 5, 514-531.
- Gau, H., Herminghaus, S., Lenz, P., Lipowsky, R., 1999. Liquid morphologies on structured surfaces: from microchannels to microchips. *Science* 283, 46-49.
- Ghaini, A., Kashid, M.N., Agar, D.W., 2010. Effective interfacial area for mass transfer in the liquid–liquid slug flow capillary microreactors. *Chemical Engineering and Processing: Process Intensification* 49, 358-366.
- Ghaini, A., Mescher, A., Agar, D.W., 2011. Hydrodynamic studies of liquid–liquid slug flows in circular microchannels. *Chemical Engineering Science* 66, 1168-1178.
- Günther, A., Jhunjhunwala, M., Thalmann, M., Schmidt, M.A., Jensen, K.F., 2005. Micromixing of miscible liquids in segmented gas–liquid flow. *Langmuir* 21, 1547-1555.
- Haase, S., Murzin, D.Y., Salmi, T., 2016. Review on hydrodynamics and mass transfer in minichannel wall reactors with gas–liquid Taylor flow. *Chemical Engineering Research and Design* 113, 304-329.
- Hartman, R.L., McMullen, J.P., Jensen, K.F., 2011. Deciding Whether To Go with the Flow: Evaluating the Merits of Flow Reactors for Synthesis. *Angewandte Chemie International Edition* 50, 7502-7519.
- Khan, W., Chandra, A.K., Kishor, K., Sachan, S., Alam, M.S., 2017. Hydrodynamics and simulation studies of liquid-liquid slug flow in micro-capillaries, 2017 International Conference on Advances in Mechanical, Industrial, Automation and Management Systems (AMIAMS), pp. 281-284.
- Kim, N., Murphy, M.C., Soper, S.A., Nikitopoulos, D.E., 2014. Liquid–liquid segmented flows in polycarbonate microchannels with cross-sectional expansions. *International Journal of Multiphase Flow* 58, 83-96.
- Kitamura, Y., Huang, Q., Miyachi, A., Yoshizako, K., Takahashi, T., 1992. Effect of temperature on interfacial tension in kerosene—surfactant—water systems. *Journal of colloid and interface science* 154, 249-254.
- Kuhn, S., Hartman, R.L., Sultana, M., Nagy, K.D., Marre, S., Jensen, K.F., 2011. Teflon-Coated Silicon Microreactors: Impact on Segmented Liquid– Liquid Multiphase Flows. *Langmuir* 27, 6519-6527.
- Lee, C.Y., Lee, S.Y., 2008. Pressure drop of two-phase plug flow in round mini-channels: influence of surface wettability. *Experimental Thermal and Fluid Science* 32, 1716-1722.
- Matsuoka, A., Noishiki, K., Mae, K., 2016. Experimental study of the contribution of liquid film for liquid-liquid Taylor flow mass transfer in a microchannel. *Chemical Engineering Science* 155, 306-313.

- N. Kashid, M., Renken, A., Kiwi-Minsker, L., 2011. Influence of Flow Regime on Mass Transfer in Different Types of Microchannels. *Industrial & Engineering Chemistry Research* 50, 6906-6914.
- Neto, C., Evans, D.R., Bonaccorso, E., Butt, H.-J., Craig, V.S., 2005. Boundary slip in Newtonian liquids: a review of experimental studies. *Reports on Progress in Physics* 68, 2859.
- Oskooei, S.A.K., Sinton, D., 2010. Partial wetting gas–liquid segmented flow microreactor. *Lab on a chip* 10, 1732-1734.
- Ou, J., Perot, B., Rothstein, J., 2004. Laminar drag reduction in microchannels using ultrahydrophobic surfaces. *Physics of fluids* 16, 4635-4643.
- Raimondi, N.D.M., Prat, L., Gourdon, C., Cognet, P., 2008. Direct numerical simulations of mass transfer in square microchannels for liquid–liquid slug flow. *Chemical Engineering Science* 63, 5522-5530.
- Raimondi, N.D.M., Prat, L., Gourdon, C., Tasselli, J., 2014. Experiments of mass transfer with liquid–liquid slug flow in square microchannels. *Chemical Engineering Science* 105, 169-178.
- Rapolu, P., Son, S.Y., 2007. Capillarity effect on two-phase flow resistance in microchannels, *International Mechanical Engineering Congress and Exposition (ASME 2007)*. American Society of Mechanical Engineers, pp. 1039-1045.
- Saien, J., Akbari, S., 2006. Interfacial tension of toluene+ water+ sodium dodecyl sulfate from (20 to 50) C and pH between 4 and 9. *Journal of Chemical & Engineering Data* 51, 1832-1835.
- Santos, R.M., Kawaji, M., 2012. Developments on wetting effects in microfluidic slug flow. *Chemical Engineering Communications* 199, 1626-1641.
- Sharma, M.K., Potdar, S.B., Kulkarni, A.A., 2017. Pinched tube flow reactor: Hydrodynamics and suitability for exothermic multiphase reactions. *AIChE Journal* 63, 358-365.
- Song, D., Daniello, R.J., Rothstein, J.P., 2014. Drag reduction using superhydrophobic sanded Teflon surfaces. *Experiments in fluids* 55, 1783.
- Srinivasan, V., Khandekar, S., 2017. Thermo-hydrodynamic transport phenomena in partially wetting liquid plugs moving inside micro-channels. *Sādhanā* 42, 607-624.
- Van Baten, J.M., Krishna, R., 2004. CFD simulations of mass transfer from Taylor bubbles rising in circular capillaries. *Chemical Engineering Science* 59, 2535-2545.
- Vandu, C.O., Liu, H., Krishna, R., 2005. Mass transfer from Taylor bubbles rising in single capillaries. *Chemical Engineering Science* 60, 6430-6437.
- Woitalka, A., Kuhn, S., Jensen, K.F., 2014. Scalability of mass transfer in liquid–liquid flow. *Chemical Engineering Science* 116, 1-8.
- Xu, J., Li, S., Tan, J., Wang, Y., Luo, G., 2006. Preparation of highly monodisperse droplet in a T-junction microfluidic device. *AIChE journal* 52, 3005-3010.
- Yuan, Y., Lee, T.R., 2013. Contact Angle and Wetting Properties. *Surface Science Techniques* 51, 3-34.

Zaloha, P., Kristal, J., Jiricny, V., Völkel, N., Xuereb, C., Aubin, J., 2012. Characteristics of liquid slugs in gas–liquid Taylor flow in microchannels. *Chemical Engineering Science* 68, 640-649.

Zhang, Q., Liu, H., Zhao, S., Yao, C., Chen, G., 2019. Hydrodynamics and mass transfer characteristics of liquid–liquid slug flow in microchannels: The effects of temperature, fluid properties and channel size. *Chemical Engineering Journal* 358, 794-805.

Zhao, B., Moore, J.S., Beebe, D.J., 2001. Surface-directed liquid flow inside microchannels. *Science* 291, 1023-1026.

Zhao, Y., Su, Y., Chen, G., Yuan, Q., 2010. Effect of surface properties on the flow characteristics and mass transfer performance in microchannels. *Chemical Engineering Science* 65, 1563-1570.